Int. J. Electrochem. Sci., 16 **(2021)** 210260, doi: 10.20964/2021.02.10

International Journal of
ELECTROCHEMICAL
SCIENCE
www.electrochemsci.org

Short communication

Solid Oxide Membrane-Assisted Controllable Electrolytic Production of TaC Nanoparticles in Molten $CaCl_2$

Kai Zheng[1,], Fanghai Lu[1], Qiong Long[1], Cuilian Shi[1], Xingli Zou[2], Zhanling Zhang[2], Xiaoling Zuo[4], Chaoyi Chen[3,*], Xiangdong Su[1,*]*

[1] School of Materials and Energy Engineering & Guizhou Key Laboratory for Preparation of Light Metal Materials, Guizhou Institute of Technology, Guiyang 550003, China
[2] State Key Laboratory of Advanced Special Steel & Shanghai Key Laboratory of Advanced Ferrometallurgy & School of Materials Science and Engineering, Shanghai University, Shanghai 200072, China
[3] School of Materials and Metallurgy, Guizhou University, Guiyang 550025, China
[4] College of Materials Science and Engineering, Guizhou Minzu University, Guiyang 550025 China
[*]E-mail: kaizhengshu@163.com (Kai Zheng); ccy197715@126.com (Chaoyi Chen); suxiangdong01@sina.com (Xiangdong Su).

Received: 4 October 2020 / *Accepted:* 19 November 2020 / *Published:* 31 December 2020

The direct electrolytic production of TaC nanoparticles from a Ta_2O_5/C precursor in molten $CaCl_2$ by using solid oxide membrane (SOM) technology was investigated in this work. A Ta_2O_5/C pellet pressed under 6 MPa was used as the cathode, and a yttria-stabilized zirconia (YSZ) tube filled with carbon-saturated liquid tin served as the anode to control the electrolysis process. The phase composition and morphology characteristics of the electrolysis products were investigated. The results show that TaC nanoparticles could be obtained directly from a Ta_2O_5/C mixture in molten $CaCl_2$ at 1000 °C and 4.0 V within 4 h.

Keywords: SOM process; molten salt; electrolysis; TaC

1. INTRODUCTION

Tantalum carbide is a typical cubic crystal carbide that is difficult to dissolve in water and organic acids, but it can dissolve in a mixture of hydrofluoric acid and nitric acid. Tantalum carbide has good conductivity and superconductivity at room temperature, and it has stable chemical properties, a high melting point and excellent oxidation resistance. TaC and Ta_2C are the common compounds formed by carbon and tantalum. The melting points of TaC and Ta_2C are 3880 and 3330 °C, respectively [1]. Because of its stable chemical properties, TaC does not react with many other chemicals and has strong oxidation resistance. However, TaC carbide is still currently produced through the traditional

carbothermal reduction method, which is an energy-intensive process. Therefore, developing an alternative process to synthesize TaC at low temperature is still needed. In 2000, Chen, Fray and Farthing successfully used solid TiO_2 powder as a raw material for the first time to produce metal Ti [2] through electrodeoxidization in molten $CaCl_2$. This method is called the FFC method, which has been demonstrated as a general process in the past 20 years for the electroreduction of solid metal oxides in molten salts to prepare metals and alloys [3-5]. The SOM method developed on the basis of the FFC method has also been proven to be used to prepare metals and alloys by using an oxygen ion-conducting inert anode [6-9]. In particular, the SOM-assisted electroreduction process has the potential to synthesize metal carbides with designed products since the carbon content can be controlled by the membrane.

In this work, we demonstrated that TaC can be directly synthesized from Ta_2O_5/C precursors in a molten $CaCl_2$ electrolyte by using the solid oxide membrane (SOM) technology. To reduce the complexity of the experiment, the Ta_2O_5/C mixture pellet is directly electrolyzed without an additional sintering process. The electrolysis process from the Ta_2O_5/C mixture to TaC is carried out at 1000 °C and 4.0 V for 4 h, and the electrolysis process as well as the obtained products are analyzed systematically.

2. EXPERIMENTAL

2.1 Fabrication of a mixed Ta_2O_5 and carbon pellet cathode

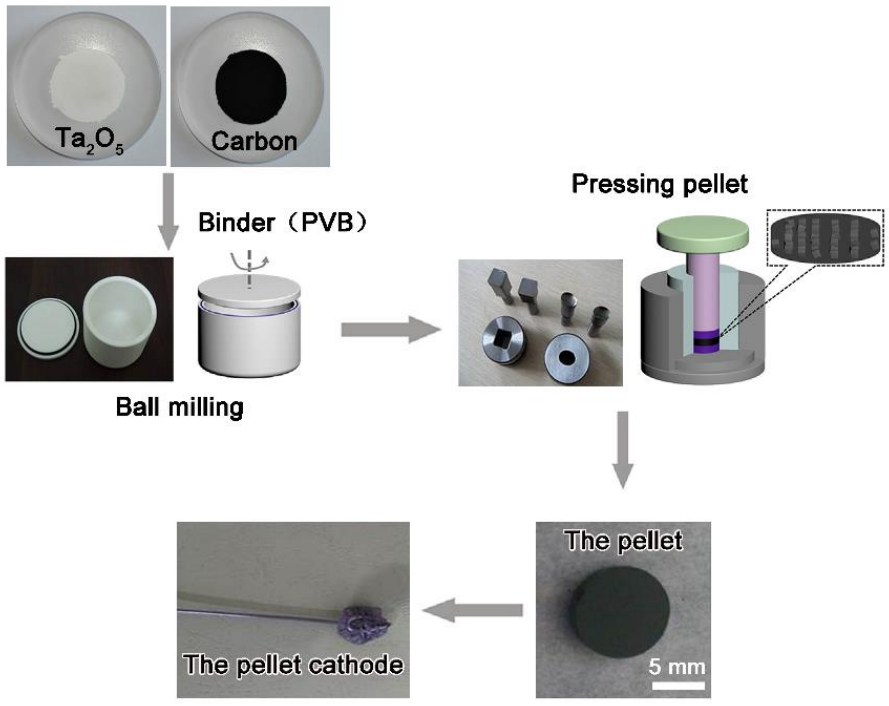

Figure 1. Schematic diagram showing the fabrication of the cathode.

Electrodes used in the present experiments included a preformed Ta_2O_5/C pellet cathode and an assembled inert SOM-based anode. A schematic diagram of the fabrication of the cathode is shown in

Fig. 1. Ta_2O_5 (Aladdin, 99.9%, average particle size ~1 μm) and carbon powder (Aladdin, average particle size ~500 nm) powders were well mixed at a molar ratio of Ta:C =1:1. The mixtures were ball milled with 2 wt.% binder (polyvinyl butyral, PVB) for approximately 24 h, and then approximately 1.0 g of the mixtures was pressed to form cylindrical porous pellet precursors (10 mm in diameter and 1.5-2.0 mm in thickness) under a pressure load of 6 MPa. The cylindrical pellet was then wrapped with two porous nickel foils (porosity:~95%, pore per inch: 110, area density: 380 g/m^2, pore size: 0.2 to 0.4 mm) and fixed on an Fe-Cr-Al wire (2 mm in diameter, as a current collector) mesh to form a pellet cathode. Porous nickel foils could be used as extended electronic conductors to provide more uniform electric contact points to the initial Ta_2O_5/C pellet precursors.

2.2 Fabrication of the SOM-based anode

A schematic diagram and photo of the fabrication of the anode is shown in Fig. 2. The assembled anode in this experiment consisted of a solid-oxygen-ion conducting membrane tube (8 mol% yttria-stabilized zirconia, YSZ; 10 mm in diameter and 100 mm in length), which was manufactured by the slip casting method in our laboratory. The YSZ tube was filled with carbon-saturated liquid tin, and an Fe-Cr-Al wire was inserted into the tube as the current conductor [10]. The carbon-saturated liquid tin was a liquid medium to transport the oxygen ions during the electrodeoxidation procedure. Considering the global emissions of CO_2, it was demonstrated in previous work that hydrogen could be introduced into the anode and react with O^{2-} to produce H_2O [10,11]. In addition, noble metals could also be painted the inner wall of the YSZ tube to oxidize O^{2-} directly to generate O_2 gas [10,12].

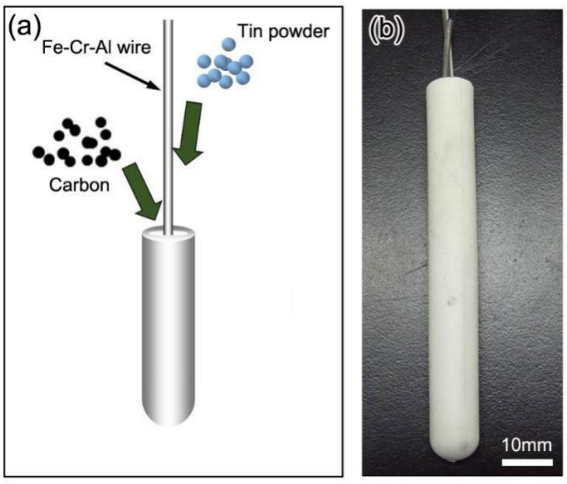

Figure 2. (a) Schematic diagram and (b) photo of the fabrication of the SOM anode (yttria-stabilized zirconia (YSZ) tube filled with carbon-saturated liquid tin).

2.3 Electrodeoxidation experiments

The assembled cathode and anode were placed in a corundum crucible that contained molten $CaCl_2$ as the electrolyte. The experiments were systematically carried out in a vertical tubular corundum

reactor located in an electrical furnace, as shown in Fig. 3. The assembled Ta_2O_5/C pellet cathode and SOM-based anode were placed in an alumina crucible. Then this alumina crucible was poured into approximately 120 g of anhydrous $CaCl_2$ powder to constitute a complete electrolytic cell. This electrolytic cell was placed in a constant temperature belt of an alumina crucible tube reactor in a tube furnace. Argon gas was continuously introduced into the reactor, and the temperature was increased to and kept at the preset electrolysis temperature (1000 °C). The experimental apparatus and the schematic of the SOM process are shown in Fig. 3. The cathode was then electrolyzed at 4.0 V for approximately 1-4 h until the current approached the background levels. A Biologic HCP-803 electrochemical workstation was connected to the anode and cathode to control the experiments and record the current-time curve during the electroreduction process. Electro-deoxidation were terminated, the obtained electrodes were removed from the molten salt into the upper part of the alumina furnace reactor and cooled naturally in a stream of argon, and then the samples were removal from the reactor and immediately washed in deionized water [10]. The morphology of the cathode samples was analyzed by X-ray diffraction using a D8 Advance X-ray diffractometer (Bruker, Germany). The microstructures of the cathode products were characterized by scanning electron microscopy (SEM, JEOL JSM-6700F). The elemental composition of the samples was characterized by using energy dispersive X-ray spectroscopy (EDS, Oxford INCA EDS system). Raman spectroscopy of the sample was performed on a Renishaw inVia Raman microspectrometer using an Ar-ion laser (633 nm).

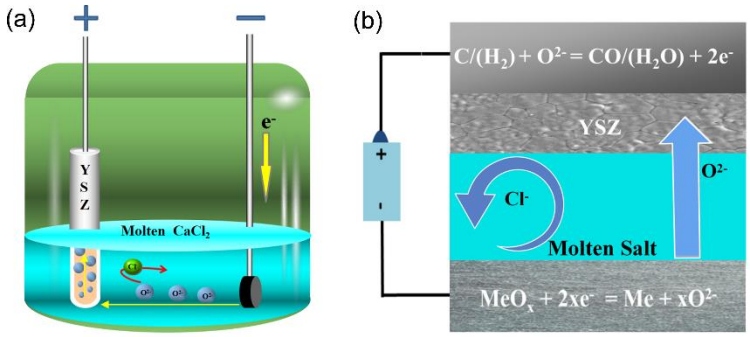

Figure 3. (a) Schematic illustration of the electrolytic cell and (b) the SOM-assisted electrodeoxidation process.

3. RESULTS AND DISCUSSION

3.1 Current-time curve of the electrolysis process

Fig. 4 presents the typical current-time curve, which was recorded during the electrochemical reduction process with the Ta_2O_5/C mixture precursor as the cathode at 1000 °C and 4.0 V. It can be seen in Fig. 4 that the current declines from approximately 1.1 A to the background levels — approximately 0.5 A in 4 h, and it is suggested that the anode system requires approximately 4 h to electrodeoxidize the pellet completely. The current during the electrochemical reduction process decreases rapidly at the beginning of electrolysis, which indicates that the electrolytic cell reaches

reaction equilibrium quickly and may be due to the initial expansion of the three-phase interlined (3PIs) metal/oxide/electrolyte on the surface of the mixed cathode [10,13,14]. Then, the current decreases slowly, which is mainly attributed to the diffusion of oxygen ions from the pellets inside to its outside through molten salt channels. As the electroreduction process continues, the oxygen component is continually removed from the mixed pellet, and the reaction interface moves into the interior of the compound pellet. When the current converges to the background levels (approximately 500 mA), it means the oxygen component contained of the Ta_2O_5/C pellet cathode has been completely reduced, and the compound pellet has been electrolyzed completely [10].

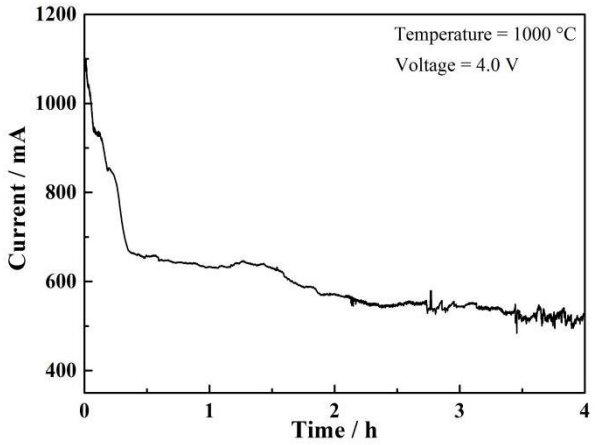

Figure 4. Current-time curve of the electrolysis process of the Ta_2O_5/C precursor.

3.2 XRD analysis of the cathodic products

The variations in the phase composition of the cathode during the electroreduction process are shown in Fig. 5. Clearly, TaC nanoparticles are successfully synthesized after 4 h of electrolysis. Fig. 5 demonstrates the XRD patterns of the products of the Ta_2O_5/C pellets after being electrolyzed for different lengths of time. Clearly, TaC can be facilely electrosynthesized from Ta_2O_5/C precursors in molten $CaCl_2$. After 1 h of reduction, diffraction peaks corresponding to $Ca_2Ta_2O_7$, TaC and $CaTa_4O_{11}$ appear. This observation demonstrates that $Ca_2Ta_2O_7$, TaC and $CaTa_4O_{11}$ are produced as intermediate products after electrolysis for 1 h. After 2 h of the reduction process, the amount of $Ca_2Ti_2O_7$ decreases gradually, while TaC and $CaTa_4O_{11}$ are continuously formed. When the electrolysis time is extended to 4 h, the product only contains a single phase TaC. It is indicated that pure TaC has been successfully produced in the cathode after electrolysis for 4 h. The electroreduction process for Ta_2O_5/C is fast, and the TaC product can remain stable during this long-term synthesis process.

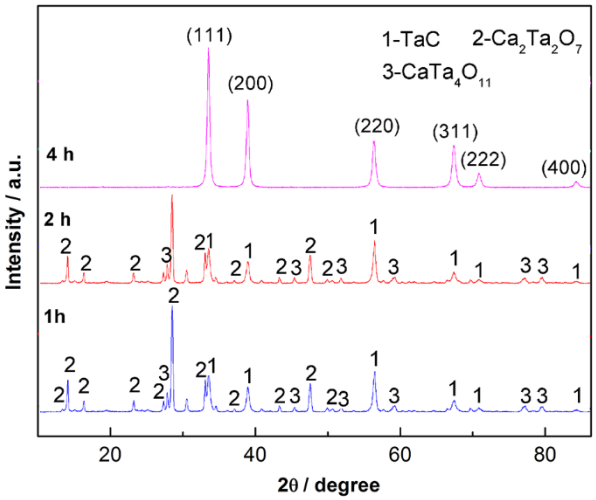

Figure 5. XRD patterns of the products of the Ta_2O_5/C pellets electrolyzed for different lengths of time.

3.3 Microstructural observations

Fig. 6(a)-(c) shows the SEM images of the cathodic products of Ta_2O_5/C pellets after being electrolyzed for different electro-deoxidation time, and Fig. 6(d) shows the EDS spectrum of the product electrolyzed for 4 h. The morphology of the cathodic product electrodeoxidized for 1 h presents a compact structure, which may be attributed to the presence of multiple products, i.e., $Ca_2Ta_2O_7$, TaC and $CaTa_4O_{11}$ (as shown in Fig. 5). With the extension of electrolysis time, the intermediate products disappear, and the final product possesses a uniform and porous structure.

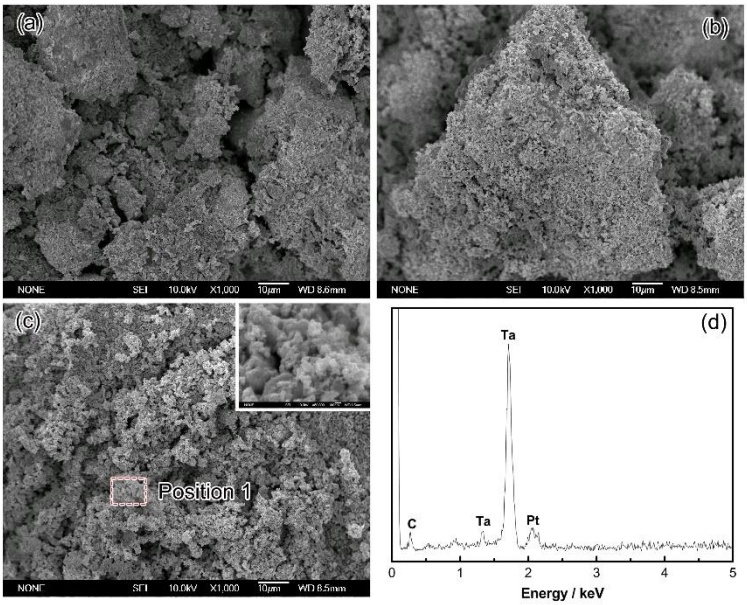

Figure 6. SEM images and EDS spectrum of the products of Ta_2O_5/C pellets electrolyzed for different times: (a) 1, (b) 2, and (c) 4 h. The inserted SEM image in (c) is the microstructure of position 1. (d) EDS spectrum of position 1.

The particle size decreases to nanoparticles after electrolysis 4 h, and the main phase is TaC. Fig. 6(c) shows the microstructure of the Ta_2O_5/C precursor after electrolysis 4 h. As exhibited in Fig. 6(c), the obtained product shows a porous structure with a particle size of ~1 μm. The EDS analysis (Fig. 6(d)) further confirms that the product only contains Ta and C. Combined with the EDS and XRD analyses, it is suggested that the synthesized product is TaC.

3.4 Raman analysis

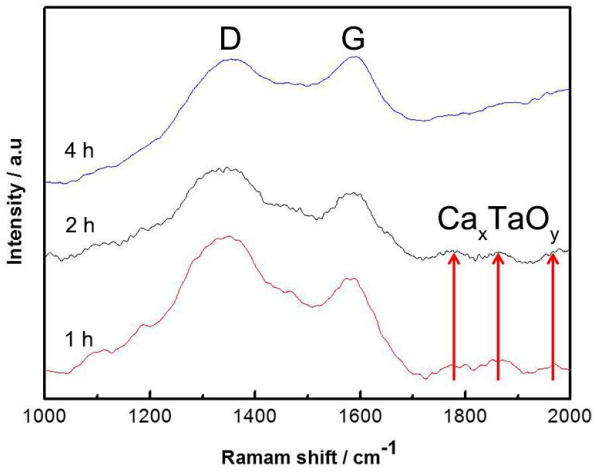

Figure 7. Raman spectra of the products of Ta_2O_5/C pellets electrolyzed for different times

Raman analysis was conducted on the obtained TaC, and the results are shown in Fig. 7. The G band at ~1345 cm^{-1} corresponds to the in-plane bond-stretching motion of carbon atoms in the sp^2 configuration with E_{2g} symmetry. The D band at ~1580 cm^{-1} is a breathing mode with A_{1g} symmetry that is forbidden in pristine graphite and becomes active in disordered graphite structures [15,16]. The ratio of the relative intensity of the D-band and G-band (I_D/I_G) represents the graphitic degree of the carbon materials [17]. As shown in Fig. 7, with the extension of electrolysis time, the intensity of the G-mode is gradually higher than that of the D-mode. It is indicated that the amount of carbon powder in the pellet cathode decreases and the degree of graphitization increases gradually. The Raman peaks at 1750~2000 cm^{-1} represent the intermediate products during the electrolysis process. The intensities of these Raman peaks decrease gradually with the extension of electrolysis time and finally disappear completely after 4 h of electroreduction. Hence, combined with Fig. 5, it is reasonable to believe that TaC powder with a relatively high purity is obtained as the final product.

3.5 Reaction mechanisms of the electrodeoxidation process

According to the results of the experiment and previous studies on the reaction mechanisms of the electrodeoxidation of Ta_2O_5 in $CaCl_2$-based molten salts [10,18], it is reasonable to believe that the reaction mechanisms of the electrodeoxidation of Ta_2O_5/C precursors to TaC in molten $CaCl_2$ generally contain chemical/electrochemical compounding, electrodeoxidation, and in situ carbonization processes

[19]. The compounding process (such as the generation of $CaTa_4O_{11}$ by the typical compounding reaction $yTa_2O_5 + xCaO \rightarrow Ca_xTa_{2y}O_{(5y+x)}$) is commonly caused by the CaO present in the molten $CaCl_2$ (without being preelectrolyzed) because CaO will be dissolved into molten $CaCl_2$ to form Ca^{2+} and O^{2-} [20]. Hence, combining Figs. 5 and 6, the reaction mechanism of the electrodeoxidation of Ta_2O_5/C to form TaC in molten $CaCl_2$ can be generally summarized as reactions (1)-(5), as illustrated in Fig. 8.

$$Ta_2O_5 + 2C + 10e^- \rightarrow 2TaC + 5O^{2-} \quad (1)$$

$$Ta_2O_5 + 2CaO\ (Ca^{2+}+O^{2-}) \rightarrow Ca_2Ta_2O_7 \quad (2)$$

$$Ca_2Ta_2O_7 + 10e^- + 2C \rightarrow 2TaC + 2CaO\ (Ca^{2+} + O^{2-}) + 5O^{2-} \quad (3)$$

$$2Ta_2O_5 + CaO\ (Ca^{2+} + O^{2-}) + C \rightarrow CaTa_4O_{11} + TaC \quad (4)$$

$$CaTa_4O_{11} + 20e^- + 4C \rightarrow 4TaC + CaO\ (Ca^{2+} + O^{2-}) + 10O^{2-} \quad (5)$$

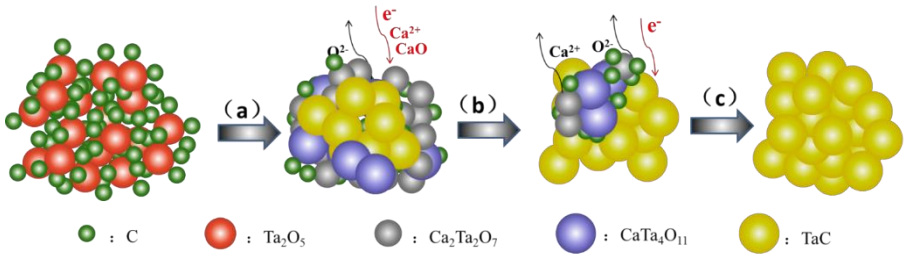

Figure 8. Schematic diagram showing the reaction routes of the electrolysis of Ta_2O_5/C to prepare TaC

4. CONCLUSIONS

In summary, TaC powders have been successfully synthesized from a mixed Ta_2O_5/C precursor at 1000 °C and 4.0 V in molten $CaCl_2$ via SOM technology. The electroreduction process was investigated by examining partially and fully reduced samples obtained at different electroreduction times. In addition, the reaction mechanism of the electroreduction process for TaC powder was discussed. The reaction pathway from Ta_2O_5/C to TaC during the electrodeoxidation process could be summarized as Ta_2O_5/C→ $Ca_2Ta_2O_7$, TaC, $CaTa_4O_{11}$ and C→TaC. The results suggested that TaC powder could be obtained as the final product with particle sizes of ~1 μm. Therefore, the SOM-assisted controllable electroreduction process has the potential to provide a novel one-step route to produce TaC powder from Ta_2O_5/C precursors in molten salts.

ACKNOWLEDGEMENTS
This work was supported by the Guizhou Province Science and Technology Planning Project (No. [2020]1Y220), the Youth Science and Technology Talent Growth Project of Education Department of Guizhou Province, P. R. China (No. [2021]264), the Research Project for High-level Talents of Guizhou Institute of Technology (No. XJGC20190960), the Overseas Talents Selection Fund of Guizhou Province, P. R. China (No. [2020]11), the National Natural Science Foundation of China (No. 51664005) and the Talent Platform [2017]5626.

References

1. O.A. Graeve and Z.A. Munir, *J. Mater. Res.*, 17(2002)611.
2. G.Z. Chen, D.J. Fray and T.W. Farthing, *Nature*, 407(2000) 361.
3. Q.S. Song, Q. Xu, X. Kang, J.H. Du and Z.P. Xi, *J. Alloy. Compd.*, 490(2010) 244.
4. Q.S. Song, Q. Xu, R. Tao and X. Kang, *Int. J. Electrochem. Sci.*, 7(2012)279.
5. J.Y. Yang, S.G. Lu, S.R. Kan, X.J. Zhang and J. Du, *Chem. Commun.*, 22(2009)3274.
6. U.B. Pal, D.E. Woolley and G.B. Kenney, *JOM*, 53(2001)32.
7. A. Krishnan, U.B. Pal and X.G. Lu, *Metall. Mater. Trans. B*, 36(2005)465.
8. X.L. Zou, X.G. Lu, Z.F. Zhou, W. Xiao and W.Z. Ding, *J. Mater. Chem. A*, 2(2014)7426.
9. X.L. Zou, X.G. Lu, C.H. Li and Z.F. Zhou, *Electrochim. Acta*, 55(2010)5175.
10. K. Zheng, X.L. Zou, X.G. Lu, S.S. Li, Y.S. Wang and Z.Y. Pang, *In TMS Annual Meeting & Exhibition. Springer, Cham.*, (2018) 481.
11. K. Zheng, X.L. Zou, X.L. Xie, C.Y. Lu, C.Y. Chen, Q. Xu and X.G. Lu, *JOM*, 70(2018) 140.
12. X.Y. Yan and D.J. Fray, *Adv. Funct. Mater.*,15(2005)1758.
13. W. Xiao, X.B. Jin, Y. Deng, D.H. Wang, X.H. Hu and G.Z. Chen, *ChemPhysChem*, 7(2006)1751.
14. V.A. Lavrenko, L.A. Glebov, A.P. Pomitkin, V.G. Chuprina and T.G. Protsenko, *Oxid. Met.*, 9(1975)171.
15. R.J. Nemanich and S.A. Solin, *Phys. Rev. B*, 20(1979)394.
16. J. Ribeiro-Soares, L.G. Cançado, N.P. S. Falcão, E.H. Martins Ferrrreira, C.A. Achete and A. Jorio, *J. Raman Spectrosc.*, 44(2013)285.
17. S. Urbonaite, L. Hälldahl and G. Svensson, *Carbon*, 46(2008)1945.
18. A. Krishnan, X.G. Lu and U.B. Pal, *Scand. J. Metall.*, 34(2005)299.
19. X.L. Zou, C.Y. Chen, X.G. Lu, S.S. Li, Q. Xu, Z.F. Zhou and W.Z. Ding, *Metall. Mater. Trans. B,* 48(2017)673.
20. X.L. Zou, K. Zheng, X.G. Lu, Q. Xu and Z.F. Zhou, *Faraday Discuss.*, 190(2016)66.